**Pergamon**

PII S1359-6462(96)00248-5

# DEFORMATION TWINS IN A SHOCK-LOADED Ta-2.5%W PRECURSOR PLATE AND A RECOVERED, Ta-2.5%W EXPLOSIVELY FORMED PENETRATOR

S. Pappu, C. Kennedy, L.E. Murr, and M.A. Meyers*
Department of Metallurgical and Materials Engineering,
The University of Texas at El Paso, El Paso, TX 79968 and
*Department of Applied Mechanics and Engineering Sciences,
University of California, San Diego, La Jolla, CA 92093

## Introduction

The effect of shock-loading on microstructural evolution and mechanical response of various metals and alloys has been studied for almost five decades [1-5]. However, BCC metals and alloys, with the exception of iron and ferritic steels, have received much less attention than have FCC materials. Recently, high density BCC materials like tantalum and tantalum-tungsten alloys have generated a lot of interest due to their armor-defeating capability in such applications as shaped charges and explosively formed penetrators (EFPs). High-explosive generated shock waves interact with the metallic liners and form these penetrators in flight. Consequently, the shock-wave parameters and initial liner microstructures can play an important role in both macro- and microstructural development of these ballistic devices.

The effects of plane-wave shock-loading as well as the subsequent plastic deformation (during EFP formation) on the microstructural evolution in Ta and Ta-W alloys have been reported by Murr and co-workers [6-11], Qiang, et al [12], and Gray and Vecchio [13]. Whereas profuse deformation twinning was seen in plane-wave shocked samples [8-11,13], there was no evidence of these features in any of the Ta EFPs [6-10,12]. Since shock-waves of higher peak pressures than necessary for plane-wave shock induced twinning are involved in EFP formation [11] it is believed that the actual, dynamic deformation process either retards or annihilates deformation twins.

In this study, we observed deformation twins in an annealed, shock-loaded Ta-2.5%W precursor plate and, for the first time, in the tail section of a soft-recovered, six-finned Ta-2.5%W EFP.

## Experimental Details

An annealed, Ta-2.5%W precursor plate 15.5 cm in diameter and 3.2 mm thick, having a Vickers hardness of 130 (200 gf load), and a true grain size (intercept length x 1.5) of 60 $\mu$m, was shock-loaded using a plane-wave focusing explosive lens arrangement [14] (using a PBX 9501 explosive main charge) which generated a plane shock wave of 45 GPa peak pressure and 1.8 $\mu$s pulse duration. The starting EFP liner

(Ta-2.5$^{w}$/$_{o}$W) was approximately 13 cm in diameter and 2.5 mm thick and was made from 4 cm diameter Cabot bar. Both the shocked plate and the EFP liner plate were orbitally forged to "pucks", then to the final discs; with one intermediate and one final anneal to produce a predominantly <100> texture. The EFP disc was also domed and machined to the final liner thickness. The true grain size was 50 $\mu$m with a Vickers hardness of 104 (1 kgf load). The warhead driving the EFP liner was a right circular cylinder, with a boat-tailed cavity, and the high explosive (H.E.) was Octol, which produced a detonation pressure of 35 GPa. Testing was done by Alliant Techsystems for the U.S. Army Armaments Research, Development and Engineering Center (ARDEC), Picatinny Arsenal, N.J. The EFP was soft recovered by firing into the Alliant Techsystems Proving Grounds "softcatch" apparatus which is similar to soft recovery systems described for shaped charge component recovery [15]. Strain rates in the EFP shock region were estimated to be ~$10^{4}$/swhile EPIC [5,16] plots employing a Johnson-Cook constitutive simulation [5,17] provided EFP half-section strain contours, with maximum true strains estimated to be 4.5 in the EFP body. Since Strutt, et al [18] have recently evaluated the role of interstitial impurities on the behavior of tantalum, it was assumed that this would also be important in these dilute alloys. The corresponding chemical analysis of the shocked plate was (in ppm): O<55, N = 20, C = 15, H<5. The corresponding chemical analysis of the EFP liner plate was (in ppm): O<50, N<10, C<10, H<10.

Specimens of the shocked sample were prepared for optical microscopy using standard metallographic practices. The etchant contained 1 mL sulfuric acid, 2 mL nitric acid, 4 mL hydrochloric acid and 16 mL hydrofluoric acid (all reagent-grade or "pure" acids). All the acids were individually cooled to 0°C before mixing one at a time, each time cooling the resulting solution back to ice temperature. Etching was also done at the same temperature. Following this, the specimens were rinsed in methanol, etched again with pure hydrofluoric acid for 10s at room temperature, and cleaned ultrasonically in methanol for 5 min.

The soft-recovered EFP was sectioned in half along the longitudinal axis and ground and polished in the usual way for optical microscopy. The etchant contained 1 mL nitric acid, 2 mL hydrochloric acid and 4 mL hydrofluoric acid (all reagent-grade or "pure" acids). Mixing and etching were done as above; no further treatment was required. Longitudinal sections were cut from the shocked plate and EFP samples and ground to about 200 $\mu$m thickness. 3 mm discs were then punched out from various sections of the EFP and the top surface of the shocked sample. TEM specimens were prepared by jet polishing in a Struers Tenupol III jet polisher using a solution consisting of 10 parts (by volume) methanol, 2 parts glycerin, 2 parts sulfuric acid, 1 part hydrofluoric acid, and 5 parts ethanol. The methanol/glycerin solution was cooled to -20°C before adding sulfuric acid to it. The resulting solution was cooled to -10°C to which hydrofluoric acid and ethanol were added. Jet polishing was done at 8-9°C and the voltage was gradually decreased from 12V to 8V during the preparation of each specimen. A Hitachi H-8000 STEM operating at 200kV in the TEM mode, and employing a double-tilt stage, was used for transmission electron microscopy.

## Results and Discussion

Figure 1 shows optical and TEM micrographs of the shocked Ta-2.5$^{w}$/$_{o}$W alloy sample. The average Vickers hardness was measured to be 311 (200 gf load). The grains show a profusion of deformation twins in various directions. The corresponding bright-field TEM micrograph in Fig. 1(b) shows twins in a grain with (100) surface orientation lying in traces of {112} planes in all four <042> directions as shown by the arrows in Fig. 1(b). The twin spots in the accompanying SAD pattern (Fig. 1(c)) coincide with the matrix spots in every third <011> layer and are therefore not apparent. Extra systematic, kinematic twin reflections are, however, seen in the SAD pattern. Extra reflections occur in the diffraction patterns because of irregular twin shapes and volumes, and often overlapping twin planes depending upon specific, operating twin shape transforms [11,19]. Figure 1(d) shows a dark-field image obtained with the objective aperture including all effective twin reflections shown by the aperture exposure zone in Fig. 1(c).
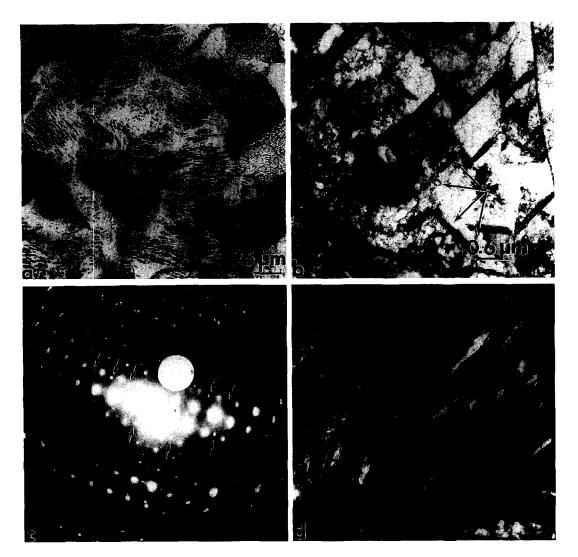
Figure 1. Optical (a) and TEM images (b and d) of a plane-wave shock-loaded Ta-2.5w/₀W sample showing deformation twins in traces of {112} planes in <042> directions, in a (100) oriented grain. Primary twin reflections coincide with the matrix spots in every third <011> layer and are not uniquely distinguished in the SAD pattern of (c). The dark-field image in (d) was obtained utilizing the reflections contained in the aperture exposure zone in the SAD pattern. Extra twin reflections are noted by arrows in (c).

Figure 2(a) shows a schematic of the EFP formation. The full view of the soft-caught Ta-2.5w/₀W EFP used for the present study is shown in Fig. 2(b). Measured Vickers hardness values over a half-section of the EFP in Fig. 2(b) varied from about 162 in the tail to 228 in the body (using a 200 gf load).

Figure 3(a) shows a bright-field TEM image of the tail section of the EFP where the true strains varied between about 1 and 2. It shows irregularly shaped (lenticular) and even cell-like deformation twins, quite unlike the ones observed in shocked Ta and its dilute alloys [8-11,13] (see also Fig. 1). The twins lie in a [1T3] direction in {2̄11} planes in a (110) oriented grain. The dark-field image using a twin and its double diffracted spot (shown circled in the SAD pattern in Fig. 3(c)) is shown in Fig. 3(b). The SAD pattern shows prominent twin reflections at <112>/3 positions. Prominent double diffraction spots are
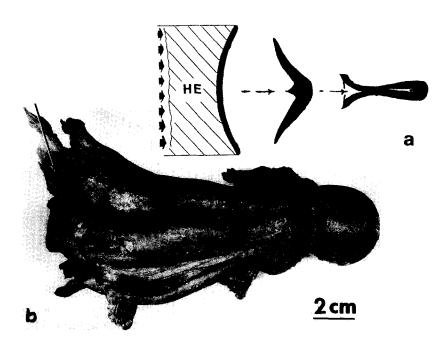
Figure 2. (a) A simple schematic representation of EFP formation; arrows indicate detonation front; (b) soft-caught Ta-2.5$^{w}/_{o}$W EFP: arrow indicates the approximate region where twins were identified in metallographic sections.

visible at 2<112>/3 positions. Extra, kinematical twin reflections due to the irregular and thin twin shapes are also present.

Figure 4(a) shows a single, small twin in a grain having a (110) surface orientation at a very high magnification. The twin boundary consists of some equi-spaced misfit dislocations primarily in the {211} planes along the long axis of the twin which are connected by a similar dislocation array composing a boundary not coincident with {211}. The twin grain has the appearance of an occlusion which may have resulted by partial annihilation (or recovery) of shock-wave induced twins similar to those in Fig. 1. Figure 4(b) shows the corresponding dark-field image utilizing the twin spot and extra twin reflections in the circled region in the SAD pattern inserted in Fig. 4(a). It may be particularly significant that unlike the shock-induced twins in Fig. 2 in the <100> texture zone, the peculiar twins in the EFP tail seem to occur prominently in (110) grains (Figs. 3 and 4).

The observation of twins in the EFP is especially interesting since no earlier studies on Ta EFPs showed any twins [6-10,12]. The lack of twins in the earlier EFPs (which experienced only slightly higher peak shock pressures of around 37 GPa using LX-14 explosive to drive them) and the nature of the twins observed in the alloy EFP in Figs. 3 and 4 may be an indication that these twins are thermally unstable, and are recovered or annihilated during the actual high strain rate deformation process (following detonation), and its subsequent temperature rise due to adiabatic heating.

Figure 5 shows some examples of an unusual occurrence of microstructure development when a thin foil of the shock-loaded Ta-2.5$^{w}/_{o}$W was heated to around 900°C in the transmission electron microscope. The lower magnification image in Fig. 5(a) shows features which differ from twins and dislocation structures shown in Figs. 3 and 4. The SAD pattern insert in Fig. 5(a) suggests that these microstructures contribute to a superlattice and are in some coincident arrangement with the Ta-W bcc structure. The enlarged image in Fig. 5(b) seems to show some kind of "domains", but their nature is not clear. Certainly these features are neither microtwins nor are they twin-related, and their identity may require more
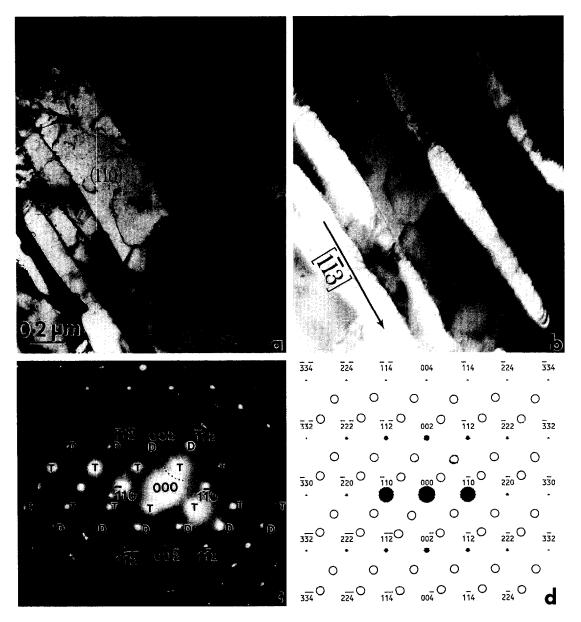
Figure 3. (a) Bright-field TEM image from the tail section of the EFP showing deformation twins; (b) dark-field image utilizing the reflections shown circled in the SAD pattern of (c) which shows prominent twin reflections, marked 'T', in <112>/3 positions. Prominent double diffracted spots, marked 'D', lie in 2<112>/3 positions. Diffraction net for a (110) oriented grain is shown in (d): Matrix reflections are denoted by • and twin reflections (primary and double diffracted) by o.

systematic and more detailed annealing experiments. That these phenomena occur at only 900°C in contrast to a melting point slightly above 3000°C in Ta-2.5$^w$/$_o$W (<0.3 $T_M$) is very interesting indeed.

Figure 4. (a) Bright- and (b) dark-field TEM images of a small twin grain in a (110) grain matrix, having an irregular, lenticular shape. Dark-field image is obtained utilizing a primary twin reflection and extra, kinematical reflections shown circled.
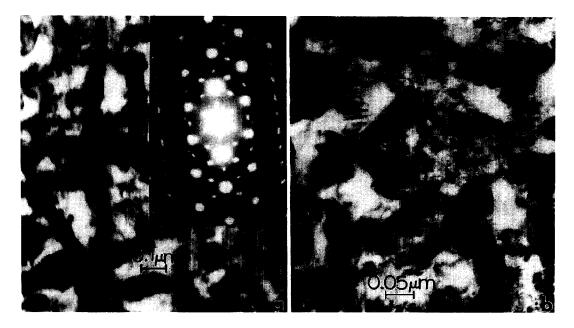


Figure 5. (a) Unknown superlattice structures created in shock-loaded Ta-2.5$^{w}$/$_{o}$W TEM specimen annealed in-situ at ~900°C. The superimposed SAD pattern shows the regular [111] matrix reflections of the form <1T0> with weaker <1T0>/2 superlattice reflections. (b) Magnified view of thermally-induced superlattice microstructure.

## Conclusions

Profuse twinning was seen in a Ta-2.5$^w/_o$W specimen subjected to a plane shock wave of about 45 GPa peak pressure and 1.8 $\mu$s pulse duration. TEM images showed twins in all four <042> directions in traces of {112} planes for (100) grain surface orientations. Twins were also observed in the tail region of a Ta-2.5$^w/_o$W EFP. These, however, had very irregular shapes and seemed to be "recovering". Owing to these features and the absence of twins in all the studies conducted thus far on Ta EFPs [6-10,12], it might be that they are very sensitive to the temperature rise associated with the post-detonation deformation. Some very preliminary, in-situ heating experiments at around 900°C have provided some rather unusual "recovery" microstructures which may or may not provide some insight into the deformation twinning dilemma.

## Acknowledgements

## References

1. L. E. Murr, Residual Microstructure-Mechanical Property Relationships in Shock-Loaded Metals and Alloys, in *Shock Wave and High Strain Rate Phenomena in Metals*, M. A. Meyers, and L. E. Murr, eds., Plenum Press, NY, 1981, p. 607.
2. L. E. Murr, Metallurgical Effects of Shock and High-Strain-Rate Loading, in *Materials at High Strain Rates*, T. Z. Blazynski, ed., Elsevier/Applied Science Publishers, NY, 1987, p. 1.
3. S. Mahajan, *Phys. Stat. Sol. (a)*, 2, 187 (1970).
4. G. T. Gray, III, Influence of Shock-Wave Deformation on the Structure/Property Behavior of Materials, in *High Pressure Shock Compression of Solids*, J. R. Asay, and M. Shahinpoor, eds., Springer-Verlag, NY, 1993, p. 187.
5. M. A. Meyers, Dynamic Behavior of Materials, John-Wiley and Sons, Inc., NY, 1994, p. 382.
6. L. E. Murr, C-S. Niou, and C. Feng, *Scripta Metall. et Mater.*, 31, 297 (1994).
7. C-S. Niou, L. E. Murr, C. Feng, and S. Pappu, *Microstructural Science*, 22, 73 (1995).
8. S. Pappu, C-S. Niou, C. Kennedy, and L. E. Murr, *Microstructural Science*, 23, (1996), in press.
9. S. Pappu, C-S. Niou, C. Kennedy, L. E. Murr, L. DuPlessis, and M. A. Meyers, in *Metallurgical and Materials Applications of Shock-Wave and High-Strain-Rate Phenomena: Proceedings of EXPLOMET '95*, L. E. Murr, K. P. Staudhammer, and M. A. Meyers, eds., Elsevier Science B.V., Amsterdam, The Netherlands, 1995, p. 495.
10. L. E. Murr, S. Pappu, C. Kennedy, C-S. Niou, and M. A. Meyers, "Tantalum Microstructures for High-Strain-Rate Deformation: Shock Loading, Shaped Charges and Explosively Formed Penetrators", paper to be presented at the Tantalum Symposium, TMS Annual Meeting, Anaheim, CA, February 4-8, 1996, and published in the proceedings: Tantalum, 1996.
11. L. E. Murr, M. A. Meyers, C-S. Niou, Y. J. Chen, S. Pappu, and C. Kennedy, "Shock-induced deformation twinning in tantalum", *Acta Materialia*, in press.
12. N. Qiang, P. Niessen, and R. J. Pick, *Mater. Sci. Engr.*, A160, 49 (1993).
13. G. T. Gray, III, and K. S. Vecchio, *Metall and Mater. Trans.*, 26A, 2555 (1995).
14. M. A. Meyers, N. N. Thadhani, and L-H. Yu, in *Shock Waves for Industrial Applications*, L. E. Murr, ed., Noyes Publications, Park Ridge, NJ, 1988, p. 265.
15. A. C. Gurevitch, L. E. Murr, H. K. Shih, C-S. Niou, A. H. Advani, D. Manuel, and L. Zernow, *Mater. Characterization*, 30, 201 (1993).
16. G. R. Johnson, Recent developments and analyses associated with the EPIC-2 and EPIC-3 codes, in Advances Aerospace Structures and Materials, S. S. Wang and W. J. Renton (Eds.), ASME, New York, 1981, p. AD-01.
17. G. R. Johnson and W. H. Cook, *Engng. Fracture Mech.*, 20 (8), 725 (1985).
18. A. J. Strutt, K. S. Vecchio, S. R. Bingert and G. T. Gray, III, Effect of interstitials on the mechanical behavior of P/M tantalum, in Tungsten and Refractory Metals, 3, MPIF, Princeton, NJ, 1995, in press.
19. L. E. Murr, Electron and Ion Microscopy and Microanalysis: Principles and Applications, 2nd Edn., Marcel-Dekker, Inc., NY, 1992.